Overview of TEXTOR Results

F.C.Schüller 2), S.S. Abdullaev 1), C.J.Barth 2), W.Biel 1), A.J.H.Donné 2), P.Dumortier 3), D.van Eester3), K.H. Finken 1), J.C.van Gorkom 2), M.von Hellermann 2), J.A.Hoekzema 1), G.M.D.Hogeweij 2), M. Jakubowski 1), R.J.E.Jaspers 2), D.Kalupin 1), M. Kobayashi 1), H.R.Koslowski 1), A.Krämer-Flecken 1), M. Lehnen 1), N.J.Lopes Cardozo 2), H.J.van der Meiden 2), A.Messiaen 3), T.Oyevaar 2), V.Phillips 1), A.Pospieszczyk 1), D. Reiser 1), D. Reiter 1), M.Z.Tokar 1), V.S.Udintsev 2), B.Unterberg 1), G.van Wassenhove 3), E.Westerhof 2), and the TEXTOR-team

Partners in the Trilateral Euregio Cluster (TEC):

1. *Institut für Plasmaphysik*, Forschungszentrum Jülich, Association FZJ-Euratom, Jülich, Germany*
2. *FOM Instituut voor Plasmafysica, Association Euratom-FOM, Nieuwegein, The Netherlands *)*
3. *Laboratoire de Physique des Plasmas-Laboratorium voor Plasmafysica, ERM-KMS, Association 'Euratom-Belgian State', Brussels, Belgiu*

e-mail: schuller@rijnh.nl

Abstract: From March 2001 to November 2002 TEXTOR undergoes a rebuild to install the Dynamic Ergodic Divertor (DED). Details of the DED will be described. During the experimental campaigns preceding the DED-shutdown the position of ITBs in L-mode-, shallow-shear- and RI-mode-plasmas were highlighted by focussed ECRH. The RI-mode can keep H-mode confinement up to N_{GW}= 1.4 provided that the neutral gas influx is kept as low as possible. The absence of power degradation in case of central ECH may be ascribed to an ITB at q=1. Impurity studies with repeated Argon puffs indicated anomalous diffusion coefficients. The impurity transport changes if the concentrations increase from 'trace' to 'bulk' levels. Observations on T_e- and n_e-fluctuations due to broadband turbulence in the presence of large m=2 islands show an enhanced fluctuation spectrum around the X-point compared to island fluctuations with improved confinement inside islands. PWI-studies concentrated on erosion/deposition of carbon, fuel recycling and retention and atomistic processes in the vicinity of limiters. The toroidal limiter is the dominant source of carbon, which is only partly re-deposited in the vicinity of the erosion. The majority is deposited at the neutraliser plates in the toroidal pump-limiters and other obstacles in the SOL. The C-layers directly facing the plasma impact have a low H-retention (< 10^{-2} H/C) due to thermal release.

1. Internal Transport Barriers (ITB)

The TEXTOR electron ITBs have been created by ECRH under various conditions: - in the current flat top phase of L-mode discharges, - in the current ramp–up phase with low or slightly negative central shear, and - in discharges of the RI-mode. It is hypothesized that the location of these transport barriers are linked to rational q-values as in the empirical q-comb model developed on the basis of RTP data. The transport is described by alternating layers of low and high electron thermal diffusivity, with e-ITBs close to low-order rational q-values. This so-called q-comb model build into the ASTRA-code gives good agreement with ECRH heated TEXTOR discharges showing in particular a clear barrier at q=1. See FIG.1 and 2. Also a barrier at q=1 might be present in RI-mode. In the latter case the barrier seems to prevent power-degradation as could be achieved by ECRH within the q=1 radius (FIG.4). ECRH at 270 kW on top of 2.7 MW NBI+ICRH power lead to a 12% increase of kinetic energy content. This augurs well for the 1 MW ECRH available in November 2002. Multiple barriers are observed in NCS-discharges (FIG.3) created by heating in the current-ramp phase. More information can be found in [1,2].

2. Improvement of RI-mode by low neutral influx

In RI-mode discharges at TEXTOR the confinement can remain at H-mode level for densities exceeding the empirical Greenwald limit by 40%. However, a successful increase of the density without confinement degradation is only obtained if the plasma density and the

neutral pressure at the edge are kept low with reduced D_2-fuelling. The causality between gas puffing and global energy content could be proven in experiments where the external gas injection rate was used to feedback control the plasma energy [3]. The higher puffing rate does not lead to higher densities because of a reduced particle confinement. The degradation occurs already at lower densities and lower puffing rates if H_2 instead of D_2 is puffed into the discharge [8]. Overall, the energy confinement time during the RI-mode stage scales with the atomic mass as $A_i^{0.5}$. A cold and dense plasma cloud at the strong and localised particle source has been found to further increase the edge turbulence [6,7].

1-D transport modelling with the RITM code was performed using anomalous transport coefficients derived for the toroidal ITG- and DTEM-modes in the plasma core and resistive ballooning instabilities at the edge [4]. The results indicate a plasma self-organisation through the interplay of different unstable modes initiated by the gas puff at the plasma edge: the increase of the edge collisionality leads to increased edge transport, increased edge transport increases the radiation efficiency $P_{rad}/(\bar{n}_e(Z_{eff}-1))$. As the radiated power P_{rad} is kept fixed in both experiment and modelling, Z_{eff} is reduced for a given $\bar{n}_e$. Z_{eff} on the other hand is the important control parameter for the transition between L- and RI-mode [5]. Consequently, once Z_{eff} gets too low in the course of the gas injection, degradation to L-mode occurs driven by an increase of the ITG mode. FIG.5 demonstrates the good agreement between the calculated radial n_e-profiles and the experimental ones in the final RI- (peaked n_e-profiles) and L-mode state (flattened profiles). A calculation of the ITG growth rates based on experimental profiles confirms the re-appearance of that mode when the degradation starts.

3. Impurity transport

Benchmarking of experimental transport data against models: Argon impurity transport has been studied in Ohmic discharges by means of a fast gas puffing technique. Applying short gas puffs to the discharge, the time evolution of spectral lines from various ionisation stages of Argon was measured using new VUV spectrometers with high time resolution. The experiments were analysed by a transport modelling (FIG.6), yielding the radial distribution of the radial diffusion coefficient D, indicating anomalously enhanced. values

The 'trace' character of impurities and the transition to bulk ion transport: The role of impurity concentration levels in ion-ion collisions is investigated in impurity scan experiments. This aspect is of particular interest for RI-mode-plasmas where in the presence of strong impurity seeding hollow impurity concentration profiles may evolve. At TEXTOR studies of neon and nitrogen scans have shown a systematic change of profile characteristics in the case when the impurity level increases from 'trace' ($c_zZ^2<<1$) to 'bulk' collisionality characteristics ($c_zZ^2\approx1$). This is a more distinct feature for Neon than for N_2 seeding**.**

4. Fluctuation spectra during MHD modes

With spectral analysis on the broadband density-fluctuations, up to 500 kHz, measured with pulse radar reflectometry in and around m=2/n=1 magnetic islands, some striking differences in the turbulence between O- and X-point could be observed [9]. The low frequency side of the turbulent spectrum was relevant down to 1 kHz as the toroidal rotation of the n=1 islands was below 100 Hz. The detailed spectra of a reflectometer channel with its reflecting density located close to the q=2 radius as shown in FIG.7, give completely different spectral shapes for fluctuations when the island or when the X-point was in front of the launcher. The latter has a much higher amplitude in the low frequencies but falling off rapidly below the island spectrum above 100 kHz. At around 200 kHz the spectral power reaches the 'noise level' of a spectrum taken from back wall reflections. For comparison, also a spectrum of a comparable discharge phase without MHD activity is shown. It is very similar to the spectrum inside the island, although at a lower value. In this particular case the density had a secondary density maximum inside the island as found by high resolution Thomson scattering. Both observations indicate that confinement inside the island is better than at the X-point.

5.Plasma Surface Interaction

Erosion/deposition of carbon and long-term fuel retention: About 2/3 of the surface of the main toroidal limiter ($3m^2$) is the dominant source of carbon, which is only partly re-deposited in the vicinity of the erosion near the limiter tip ($1m^2$). A large majority (>90%) of the carbon is deposited at the plasma facing side of the neutraliser plates in the 8 toroidal pump-limiters (0.2mg/sec) and other obstacles in the SOL. The formed hydrocarbons are pumped out. The transport in the vicinity of the targets is modelled with a Monte Carlo code in which new data on sticking probabilities, an improved set of hydrocarbon rate coefficients. and carbon recombination rate coefficients have been implemented. Chemical erosion yields of about 20% are necessary to describe the deposition efficiencies. The re-deposition efficiency of ^{13}C-marked methane injected through limiters has been measured and modelled. A very low re-deposition has been detected (<1 %) compared with the predictions from modelling using standard erosion and sticking values (50%). However with a high chemical re-erosion (10-20%) of the freshly deposited hydrocarbon species together with low sticking factors experimental results can be simulated. Under these conditions the C-layers facing the plasma have a low H-retention ($< 10^{-2}$H/C) due to thermal release.

Atomistic processes of hydrogen recycling in the vicinity of limiters: Fulcher-band spectroscopy of hydrogen molecules has been developed as a method to determine which fraction of the hydrogen is being recycled as atoms or as molecules. The method also answers the question whether the molecules and atoms leave the surface in an excited energy state. Excited molecules might undergo different ionization processes compared to those in the ground state. Strong coupling between the molecular rotational and vibrational temperatures was found. Molecular particle fluxes in the order of several $10^{20}m^{-2}s^{-1}$ were measured in front of a graphite test limiter, located at the LCFS. The increase of these fluxes with the local plasma edge parameters was verified by means of the MC code EIRENE. The velocity distributions of atomic deuterium have been measured *in situ* in front of the graphite test limiter by VUV laser-induced fluorescence with variable surface temperatures up to 1000 ^{0}C. A strong thermal component in the distribution was revealed.*More details will be given in another contribution to this conference* [10]

6. DED issues

The set-up: The installation of Dynamic Ergodic Divertor (DED) in the TEXTOR vessel has just been finished. See FIG.8. The currents (<15 kA) in the set of 16 magnetic perturbation coils (4 quadruples) plus 2 compensation coils ergodize the magnetic field structure in the plasma edge region. They are located inside the vacuum vessel at the high field side of the torus at a minor radius of r_{coil} = 0.5325 m. The individual perturbation coils follow the direction of the q=3 equilibrium magnetic field near the plasma edge helically once around the torus. The.perturbation modes (m=10...14, n=4) create chains of magnetic islands destroying the resonant magnetic surfaces.

Characteristic edge structures created by ergodization: Field line tracing and mapping are used for finding the topology of the structures in the perturbed magnetic field [11,12]. The flux surfaces inside q(r) =2, remain nearly undisturbed. Further outwards islands develop and grow; finally, different islands overlap and form an ergodic sea, destroying the magnetic surfaces. Variation of q_{edge} will shift the resonant radius and the ergodic zone radially in the range $0.9 \leq r/a \leq 1$ keeping the Chirikov parameter above 1. Adjustment of the individual coil currents allows the superposition of different base modes [13].

The magnetic field lines, in the outermost so-called *laminar zone* [14], intersect the divertor target plate with a connection length between two intersections with the wall comparable to or smaller than the Kolmogorov length (typically some 10 m). Here the transport changes from a diffusive character to a convective one with plasma streaming to the plasma facing components as in the conventional scrape-off layer

Dynamic aspects: Static DED operation will guide the heat flux towards fixed strike zones on the divertor target plate following helically the DED coils. Dynamic DED operation will

spread the heat load over the whole target area. In cylindrical approximation [15] it has been shown that the „low frequency“ (relative to Ω_i) electromagnetic waves of the DED effectively propagate in the area between coils and resonance layer as compressional Alfvén (fast) waves [16]. The interaction of the rotating field with the current driven in the shielding layer results in the transfer of large toroidal and poloidal angular momentum between DED-coil and plasma.

7. References

[1] E.Westerhof et al.,. Proc. of the EC-12 Workshop in Aix-en-Provence, France (May 2002)
[2] F.C. Schüller et al., Proc.28th EPS Conf. on Plasma Phys. Control. Fus., Funchal (2001), ECA 25 A, 1.
[3] A. Messiaen et al., Proc. 28th EPS Conf. on Plasma Phys. Contr. Fus., Funchal (2001), ECA 25 A, 81
[4] D. Kalupin et al., Plasma Phys. Control. Fusion 43 (2001), 945.
[5] M.Z. Tokar', J. Ongena, B. Unterberg, R.R. Weynants, Phys. Rev. Lett. 84 (5) (2000), 895.
[6] D. Reiser, M.Z. Tokar' and B. Unterberg, contr. to the 15th Int. Conf. on Plasma Surface Interaction, Gifu City, Japan, May 2002, accepted for publication in J. of Nucl. Mater.
[7] M.Z.Tokar’ et al., contr. 29th EPS Conf. Plasma Phys. Contr. Fus., Montreux (2002)
[8] G. Van Wassenhove et al , contr. 29th EPS Conf. Plasma Phys. Contr. Fus., Montreux (2002)
[9] J.C.van Gorkom et al., Proc. 28th EPS Conf. Plasma Phys. and Contr.Fus., Funchal, (2001)
[10] V.Philipps et al., contribution EX/P5-08 to this conference
[11] S.S. Abdullaev et al., Phys. Plasmas, 5 (1998) 196
[12] Abdullaev, S.S., Finken, K.H., Spatschek, K.H., Phys.Plasmas, 6 (1999) 153
[13] Finken, K.H., Abdullaev, S.S, Kaleck, A., Wolf, G.H., Nucl. Fusion, 39 (1999) 637
[14] Th. Eich, D. Reiser, K.H. Finken, Nucl. Fusion, 40 (2000) 1757
[15] Finken, K.H., Nucl. Fusion, 30 (1999) 707
[16] Faulconer, D.W., Koch, R., Fusion Engineering and Design, 37 (1997) 399

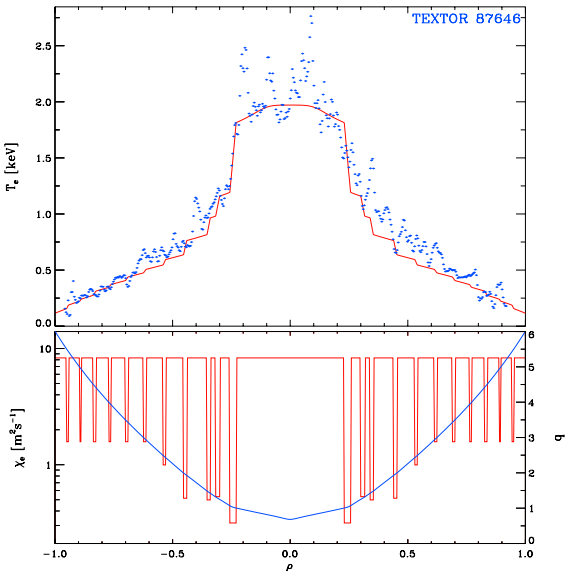

FIG.1 The T_e profile in a discharge with central ECRH simulated with the RTP q-comb model for the electron heat conductivity. P_{ECRH} = 250kW. Blue dots 1 Blue dots represent T_e measured by Thomson scattering. The red curve gives the result of the simulation. The bottom panel shows the q profile (blue) and the corresponding profile of the electron heat conductivity (red).

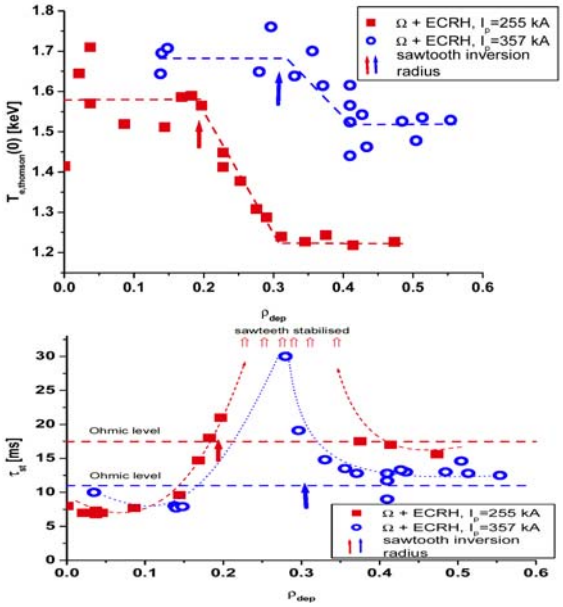

FIG. 2. Top: the central T_e (Th.sc). and the corresponding sawtooth period (bottom) achieved in Ohmic discharges with ECRH (270 kW) as a function of the ECRH deposition radius. Blue squares for 255 kA and red circles for 357 kA. In the lower current case sawteeth are stabilized, when ECRH is deposited within a region just outside the sawtooth inversion radius ranging from ρ_{dep} = 0.23 to 0.35.

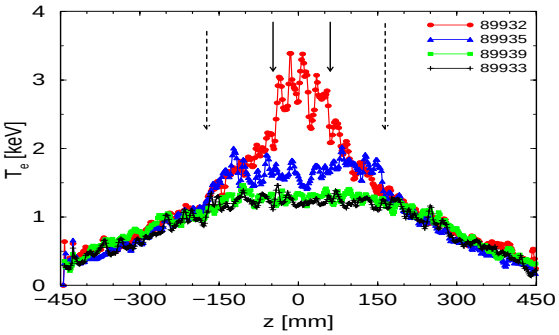

FIG.3. T_e profiles from Thomson scattering during the current ramp-up phase (NCS)and P_{NBI}= 1 MW counter for different ECRH (250 kW) depositions at r/a=0.06 (red), 0.23 (blue), 0.5 (green) and NBI-only (black).A double ITB (arrows) is clearly visible

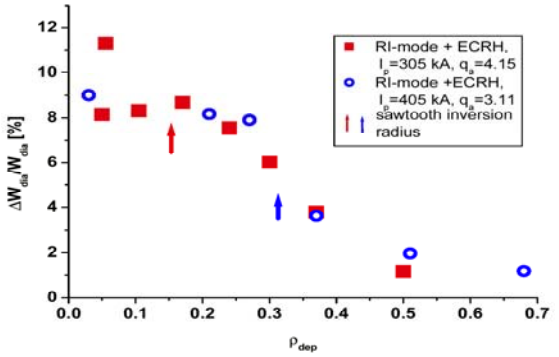

FIG.4. The normalised increse of normalised energy content duringRI-mode due to a 10% increase in power by ECRH as function of the deposition radius. Arrows indicate r(q=1).

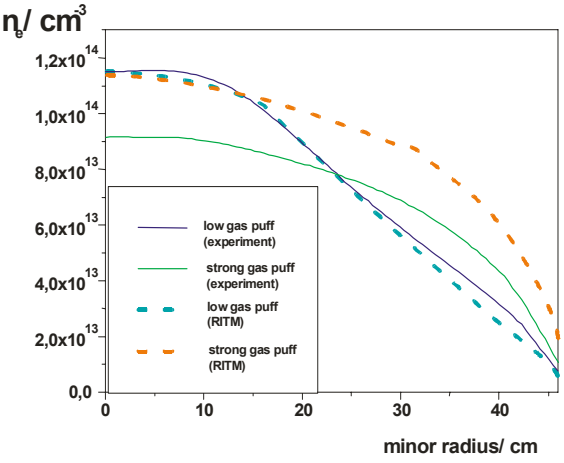

FIG.5. Experimental(solid) and calculated (dashed) density profiles for high-density RI-discharges with low and strong gas fuelling

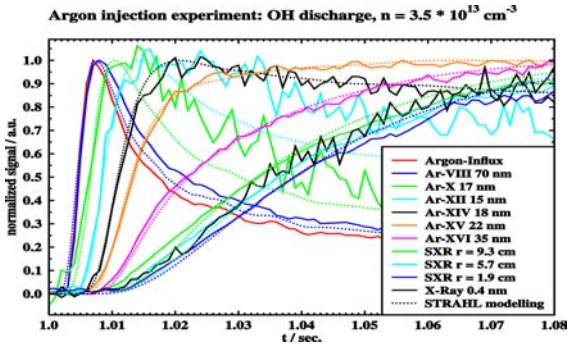

FIG.6 VUV transport studies with enhanced time resolution. The modeling of the impurity time traces representing several ion stages of argon by transport code STRAHL allows the deduction of particle diffusion coefficients

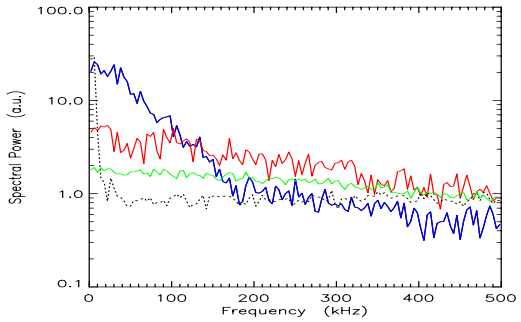

FIG.7. The density fluctuation spectra measured with pulse radar reflectometry at the O-point of a large m=2 island (red);at the X-point of the same mode (blue); at a comparable L-mode plasma without islands (green) and the detection noise (black)

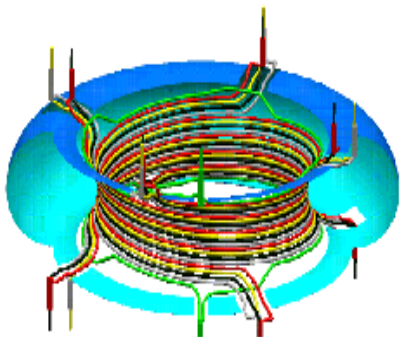

FIG 8. Schematic view on the location of the perturbation coils of the DED. 16 coils are helically wound around the torus at the high field side. The four different colours represent the phase distribution of the perturbation current in the 12/4 base mode.